On the Physical and Chemical Consequences of Lunar Picritic Magma-Anorthosite Reaction. Y. Liang, Z. Morgan, & P. Hess, Brown University, Dept. of Geological Sciences, Providence, RI 02912, yan_liang@brown.edu.

Physics: Lunar picritic magmas must pass through the thick anorthite-rich crust (anorthosite, troctolite, and norite) to be erupted on the surface. Given the large thermal and chemical differences between the picritic melts and the lunar crust, it is inevitable that melt-rock reaction takes place during magma transport through the crust. Figure 1 illustrates the essential features of melt-rock reaction in the lunar

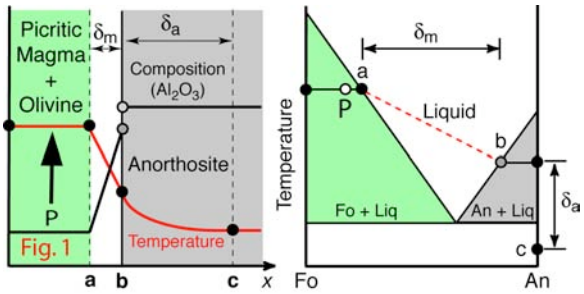

crust. It involves both melting and dissolution. As hot olivine-bearing picritic magma (P in Fig. 1) travels through lunar crust, via large dikes, say, it losses heat to the wallrock, resulting in wallrock melting [1]. Addition of anorthite-rich components to the reacting magma lowers olivine liquidus temperature, which suppresses olivine crystallization and dissolves existing olivine in the picritic magma, provided the heat flux brought by the melt is sufficiently large to maintain the temperature above the olivine-anorthite cotectic at $x = b$ in Fig. 1. Hence a crystal-free thermo-chemical boundary layer δ_m is developed on the melt-side of the melt-rock interface and a thermal boundary δ_a on the rock-side of the interface (Fig. 1). The large temperature and concentration gradients within δ_m suggest that both melting and dissolution play an important role in anorthosite assimilation. The rate of melt-rock reaction in this case is determined by how fast the melted/dissolved anorthosite components can be transferred across the boundary layer δ_m, where the thickness of δ_m depends on conduit geometry, vigor and styles of convection in the picritic melts.

In a preliminary study we examined the rates of anorthosite diffusive and convective dissolution in an Apollo 15 green glass at 1400°C and 0.6 GPa and found very fast anorthosite dissolution rates in this melt [2]. Fig. 2 shows even faster anorthosite diffusive (hence convective) dissolution rates in a red and yellow glass at the same *P-T*, with the red glass having the highest dissolution rate (experimental method is on the next page). The high dissolution rates is due to a combined effect of faster chemical diffusion in the low viscosity melts and greater extent of undersaturation between the anorthite and picritic liquids [2]. It suffices to say that melting and melt-rock reaction is capable of assimilating significant amounts of lunar crustal materials into picritic magmas.

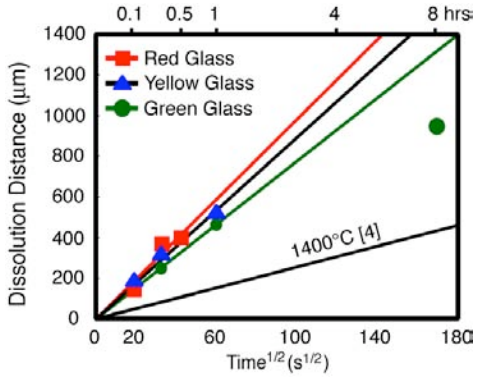

Fig. 2. Summary of anorthosite dissolution runs. Symbols represent measured dissolution distances. Dissolution experiments were conducted at 1400°C and 0.6 GPa following the procedures described in [2, 3]. Lower solid line is from plagioclase dissolution experiment of [4] at 1400°C and 1 atm.

The physical and chemical properties of the melt within δ_m are essential in understanding the consequences of picritic melt-anorthosite reaction in the lunar crust. To a first approximation, we can estimate the melt compositions within δ_m, which is also a function of *P-T*, using the anorthosite-picritic melt dissolution experiments reported in Fig. 2.

Chemistry: Melting or dissolution of anorthosite primarily adds CaO and Al_2O_3 to the picritic melts, diluting the abundance of MgO, FeO and other elements not contained within anorthosite while leaving the Mg# of the melt largely unchanged. Fig. 3 displays the correlations of CaO and Al_2O_3 in melts from three of our anorthosite dissolution experiments (in red, yellow, and green glasses, small black symbols). As expected, the melt compositions at the anorthosite-melt interface are strongly enriched in Al_2O_3 (30.8-33.8wt%) and CaO (13.3-13.9%), resulting in very large Al_2O_3 and CaO concentration gradients at the melt-rock interface (Fig. 1), and hence very fast anorthosite dissolution rates in these melts. Because chemical diffusion rate of CaO in the melt is different from that of Al_2O_3, the concentration paths are characteristically nonlinear in this plot, i.e., diffusion-assisted mixing path in composition space is different from simple mechanical mixing path within the concentration boundary layer (δ_m in Fig. 1). Fig. 3 (and Fig. 4) shows that anorthosite

assimilation, via melting and dissolution, is capable of producing the observed CaO and Al_2O_3 variations in the picritic glasses, consistent with the conclusion of Jones and Delano [5].

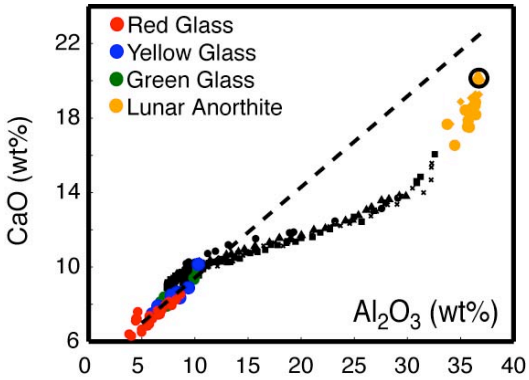

Fig. 3. Comparison of CaO and Al_2O_3 in the picritic glasses (red, blue, and green symbols, [6, 7]) with our measured dissolution profiles (black symbols). Dashed line is the linear extrapolation of the green glass data. Orange symbols are lunar plagioclase [8, 9] and open circle is pure anorthite.

Fig. 4 further explores the effect of Al_2O_3 addition during anorthosite dissolution. While the differences in TiO_2 abundance among the three picritic glasses are unrelated to Al_2O_3 addition, the locations of the high-Al basalts (light blue field) in this and other oxide correlation diagrams are intriguing, begging the question if the high-Al basalts were produced by reaction between picritic magmas and anorthite-rich lunar crust. Origins for the high-Al basalts include either impact melting on the lunar surface [10], or small degrees of melting of troctolite, plagioclase-bearing werhlite, or harzburgite [11, 12], followed by KREEP assimilation and fractional crystallization [13, 14]. Although the melt-rock reaction origin for the high-Al basalts can also explain the very old age of the high-Al basalts, it is by no means definitive. An important question is how to get the reacted melts to the surface while still preserving their unique geochemical signatures.

How to get them out: Melt-rock reaction occurs at magma-wallrock interface and hence is a local phenomenon. Given the highly turbulent nature of convective flow in large magma conduits, it is virtually impossible to prevent the reacted melt within δ_m from mixing and mingling with the through-going picritic magmas, especially at greater depth. At shallower depth or near surface conditions where the distance over which the melts have to travel is small, mixing and mingling between the reacted and unreacted melts may not be complete for two reasons: (1) the densities (viscosities) of the high-Al_2O_3 melts within δ_m are smaller (larger) than those of the unreacted picritic magmas, making them easier to separate or detach from the boundary layer; and (2) the segregated melts will have a better chance at least to partially preserve their chemical identify if the size of the magma conduit is small and the geometry of the conduit is not vertical, i.e., a side branch of the main dike. Hence the volume of the partially preserved melts is likely to be very small. Clearly more detailed calculations are needed to further quantify this model.

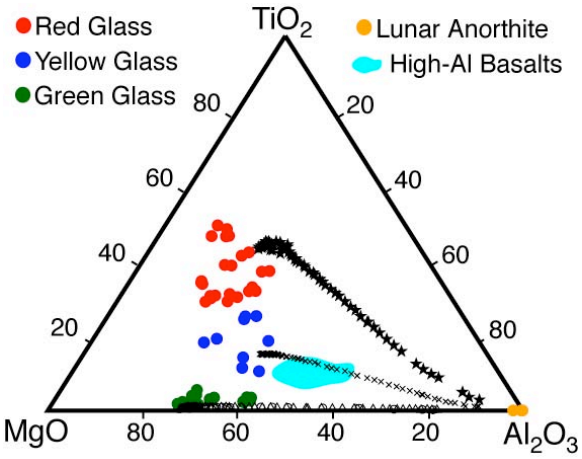

Fig. 4. Comparison of MgO-Al_2O_3-TiO_2 in lunar picritic glasses [6, 7] and high-Al basalts [11, 13] with our measured dissolution profiles. Symbols are the same as in Fig. 3. Oxide abundance is re-normalized to 100% in this plot.

Experiments characterizing the kinetics of anorthosite dissolution in three Apollo 15 green glass (5C, [6]), yellow (2C, [6]), and red glasses (group A, [15]) were carried out at 1400°C and 0.6 GPa using the dissolution couple method [2, 3]. Dissolution couples were formed by juxtaposing pre-synthesized green, yellow, or red glass and pre-synthesized anorthosite in graphite lined Pt-Mo capsule and ran for 0.1 to 8 hrs. Starting materials were synthesized from oxide mixtures and an anorthite glass powder.

References: [1] Finnila et al. (1994) *JGR 99*, 14,677-14,690. [2] Morgan et al. (2003) *LPSC* XXXV #1830. [3] Morgan and Liang (2003) *EPSL 214*, 59-74. [4] Tsuchiyama (1985) *CMP 89*, 1-16. [5] Jones and Delano (1989) *GCA, 53*, 513-527. [6] Shearer and Papike (1993) *GCA, 57*, 4785-4812. [7] Elkins et al. (2000) *GCA, 64*, 2339-2350. [8] Papike et al. (1996) *GCA, 60*, 3967-3978. [9] Shervais and McGee (1998) *GCA, 62*, 3009-3023. [10] Snyder et al. (2000) In: *Origin of the Earth and Moon*, Canup and Righter, eds., Univ. of Arizona Press, pp361-395. [11] Dickinson et al. (1985) *Proc. 15th LPSC*, 2, C365-C374. [12] Ridley (1975) *Proc. 6th LPSC*, 131-145. [13] Neal et al. (1989) *Proc. 19th LPSC*, 147-161. [14] Neal and Taylor (1990) *Proc. 20th LPSC*, 101-108. [15] Delano (1980) *Proc. 11th LPSC*, 251-288.